Measuring the Cosmic Equation of State with Counts of Galaxies II: Error Budget for the DEEP2 Redshift Survey

Jeffrey A. Newman and Marc Davis[1]
Department of Astronomy, University of California, Berkeley, CA 94720-3411
jnewman@astro.berkeley.edu, marc@astro.berkeley.edu

ABSTRACT

In a previous paper, we described a new variant on the classical "dN/dz" test which could be performed using data from the next generation of redshift surveys. By studying the apparent abundance of galaxies as a function of their circular velocity or velocity dispersion, rather than luminosity, it is possible to avoid many of the uncertainties of galaxy evolution while using quantities that may be measured directly. In that work, we assumed that counting statistics would dominate the resulting errors. Here, we present the results of including cosmic variance and determine the impact of systematic effects on attempts to perform the test with the upcoming DEEP2 Redshift Survey. For the DEEP2 survey geometry, cosmic variance yields errors roughly twice those predicted from Poisson statistics. Through Monte Carlo simulations we find that if the functional form, but not the strength, of any of the major systematic effects (baryonic infall, velocity errors, and incompleteness) is known, the free parameter may be determined from the observed velocity function. The systematic may then be corrected for, leaving a much smaller residual error. The total uncertainty from systematics is comparable to that from cosmic variance, but correlated amongst redshift bins. Based on these analyses, we present error budgets for a dN/dz measurement with DEEP2 and determine the resulting constraints on cosmological parameters. We find that the uncertainty in the cosmic equation of state parameter w are $\sim 2\times$ higher than previously derived, providing a measurement much stronger than any available today but weaker than some other proposed tests.

Subject headings: cosmological parameters, cosmology: observations, galaxies: high-redshift,galaxies: fundamental parameters

1. Introduction

In a previous paper (Newman & Davis 2000, hereafter ND00), we described a new variant on the classical "dN/dz" test which could be performed using data from the next generation of redshift surveys. This classical technique determines the evolution of the cosmic volume element by measuring the redshift distribution of a tracer whose number density is known, providing constraints on fundamental cosmological parameters. In the past, the abundance of galaxies was used to perform this test under the assumption that the total comoving number density of galaxies integrated over all luminosities is independent of redshift (with further assumptions about the luminosity function; e.g. Loh & Spillar 1986). Such assumptions may be suspect, but improving upon them would require a reliable, comprehensive theory of galaxy formation and evolution.

Instead, ND00 suggests that by measuring the apparent abundance of galaxies as a function of their linewidth or velocity dispersion (normalized to the abundance at $z \sim 0$), it is possible to obtain a more reliable measurement of the volume element, exploiting the simplicity of the dark matter halo velocity function. Current and upcoming large redshift surveys with moderately high spectroscopic resolution will make this possible.

[1]Also Department of Physics, U.C. Berkeley

The DEIMOS/DEEP Redshift Survey (hereafter, "DEEP2") is particularly well suited for the technique. This project is a major effort to observe distant galaxies using the new DEIMOS spectrograph on the Keck telescope, scheduled to be installed in early 2002. Its goal is to obtain high quality spectra of 50,000 galaxies selected to have minimum redshift $z > 0.7$ (the "1HS", or 1-hour survey, so named because of the expected exposure time per slitmask) and spectra of 5,000 such galaxies in selected regions to a fainter limiting magnitude (the "3HS", or 3-hour survey). DEEP2 will obtain data characterizing galaxies and large-scale structure at $z \sim 1$ comparable in quality to what is currently available for $z = 0$. Although we have much information on the local universe, we know little about how it has reached its present state; this survey has been designed to address this major gap in our knowledge.

In our previous work, we assumed that the uncertainties in a $\mathrm{d}N/\mathrm{d}z$ measurement using DEEP2 would be dominated by Poisson statistics and found that it could provide strong constraints on the cosmic equation of state parameter of quintessence-like models, $w = P/\rho$. Because the velocity function of dark matter halos is so simple (a nearly perfect power-law at galactic scales), we presumed that any systematic effects would leave a clear signature and could be removed or avoided, and that counting statistics would therefore dominate the uncertainties. However, we did not consider the fundamental limit to the accuracy of any count imposed by cosmic variance. In this paper, we calculate its impact on the DEEP2 survey.

Since ND00, a number of papers suggesting that systematic effects would compromise our proposed test have appeared in the literature (e.g. Bullock et al. 2000), though again without actually evaluating their impact on realistic methods of measuring $\mathrm{d}N/\mathrm{d}z$. This paper addresses that gap in our previous work; we have performed quantitative tests of the impact systematic effects should have on our ability to measure $\mathrm{d}N/\mathrm{d}z$ with DEEP2. However, we must do so without the information that will be available at the completion of the survey. For instance, semi-analytic and N-body estimates of the impact of baryonic infall on the potential well depths of galaxies are still developing (e.g. Kochanek & White 2001), and comparisons between HI rotation curves and O[II] linewidths for DEEP2 galaxies may be possible in the future, but are unavailable to us now.

Rather than attempting to foresee all that the next few years will bring, we have instead chosen to evaluate the impact of major systematic effects by applying "toy" models of their impact to a semi-analytic prediction of the dark-matter halo velocity function (a la ND00). The semi-analytic methods used duplicate the general behavior seen in N-body simulations. The toy models used each have one free parameter that is treated as unknown going into the analysis. We then generate Monte Carlo realizations of the velocity function affected by these model systematics and determine the resulting errors in measuring both the free parameter and the abundance of dark halos in such datasets. Thus, for any value of the free parameter we can determine the excess variance in a $\mathrm{d}N/\mathrm{d}z$ measurement due to the residual uncertainty from that systematic effect after removal. So long as the toy models duplicate the major features of the real systematics, we should obtain reasonable estimates of the actual errors from DEEP2. In § 2 of this paper, we calculate the impact of cosmic variance; in § 3, we determine the residual errors that will result from systematic effects; and in § 4, we present the constraints on cosmological parameters that a measurement of $\mathrm{d}N/\mathrm{d}z$ from the velocity function of DEEP2 galaxies would provide.

2. Cosmic Variance

By definition, the spatial correlations of galaxies imply that they are not distributed independently and thus cannot obey simple Poisson statistics. Instead, in a given volume there will be an excess variance

$$\sigma^2_{CV} = \frac{1}{V^2} \int_V \xi(x_1, x_2) d^3x_1 d^3x_2, \qquad (1)$$

where ξ is the two-point correlation function of galaxies and V is the volume in which we wish to calculate the variance. This integral may more easily be evaluated in Fourier space, where we obtain

$$\sigma^2_{CV} = \frac{1}{8\pi^3} \int P(k) |\tilde{W}(k)|^2 d^3k, \qquad (2)$$

where $\tilde{W}(k)$ is the Fourier transform of a spatial window function that is 1 inside the volume and

zero elsewhere and $P(k)$ is the power spectrum of the galaxy distribution. To evaluate the integral, we use the CDM-like power spectrum of Bardeen et al. (1986) with $\Gamma = 0.25$ and slope $n = 1$, consistent with recent observations.

We are interested specifically in the effect of cosmic variance upon measurements of $\mathrm{d}N/\mathrm{d}z$ with DEEP2 (as the volume observed in the next generation of $z \sim 0$ surveys is much greater, cosmic variance in local comparison samples should be comparatively negligible). Because the CFH12k camera used in imaging has a $30' \times 40'$ field of view, the most efficient geometry for each of the four fields to be surveyed (Davis & Faber 1998) is one which is $30'$ in the shortest direction. Based on observing time constraints, we further expect each field to cover $120'$ in the long direction on the sky; the required imaging is nearly complete. If we assume an Ω_m=0.3 ΛCDM model, this corresponds to $20.2 \times 80.8 h^{-1}$ Mpc comoving at $z = 1$, the expected median redshift for the survey. We have calculated the cosmic variance for each field assuming that the volume surveyed is a rectangular solid extending 1300 h^{-1} Mpc comoving in the redshift direction (corresponding to $0.7 < z < 1.5$).

For a rough estimate, we could assume that the power spectrum of galaxies has the same normalization as clusters today, applying the σ_8 measurement of Borgani et al. (1999), which yields 0.96 for an $\Omega_m = 0.3$ LCDM model (for quintessence models, we use the relations of Wang and Steinhardt (1998) with $\Theta = 0.075$). We then find that the uncertainty in a density measurement will be 5.9% in each of the four fields, or 2.9% for the entire survey (as the fields are widely spaced on the sky, there should be minimal correlation between them at $z = 1$, so the combined variance goes as $1/N_{fields}$).

However, to calculate the variance in counts of galaxies, we must use the power spectrum of galaxies at $z = 1$ rather than clusters at $z = 0$; we therefore must renormalize to match σ_8 for galaxies. A measurement of the correlation length r_0 may be directly transformed into a measurement of σ_8 if the correlation index γ is known (Peacock 1999); however, the correlation properties of galaxies at $z \sim 1$ remain poorly known. Observations suggest that $r_0 \sim 2.5h^{-}1$ Mpc (comoving; see Hogg et al. 2000), similar to the correlation length of the dark matter at that redshift, but semi-analytic models predict $r_0 \sim 4h^{-1}$ Mpc (comoving) for luminous galaxies at that redshift (Benson *et al.* 2001). For $\gamma = 1.8$ and $r_0 = 2.5, 3.25, 4$, $\sigma_8 = 0.474, 0.600, 0.723$. Thus, we expect cosmic variance in the DEEP volume to be somewhat lower than a naive calculation would yield: 1.4 – 2.2 % rather than 2.9%. Since DEEP2 will obtain linewidths for $\sim 10^4$ galaxies with linewidths, the uncertainty due to cosmic variance will be roughly twice the Poisson value. In Figs. 1 and 2, we show the effect of changing the survey geometry or areal coverage on the cosmic variance in overall DEEP2 results. The amount of area surveyed on the sky is clearly of greater importance than the shape of the surveyed region.

Cosmic variance need not impose a permanent limit to the precision of a DEEP2 $\mathrm{d}N/\mathrm{d}z$ measurement; if imaging of a wider area is available sufficient to produce an accurate photometric redshift distribution (even if information on individual galaxies remains uncertain), it could be possible to renormalize the total abundances of galaxies in the DEEP2 fields and reweight the abundances of galaxies with observed linewidths. Other redshift surveys extending to $z \sim 1$, particularly the VLT/VIRMOS survey, could also provide corrections. However, cosmic variance would almost certainly remain an insurmountable obstacle to efforts to measure the evolution in the equation of state parameter w via DEEP2 $\mathrm{d}N/\mathrm{d}z$ alone, since the variance is higher in any subvolume than for the survey as a whole.

3. Correction for systematic effects

Like most astronomical studies, the measurements proposed by ND00 could be subject to a number of systematic effects. If these systematics are well-understood and their magnitude is known, it is straightforward to correct for them when measuring the halo velocity function. However, few, if any, of the systematic effects that will affect this measurement can yet be predicted accurately. For instance, we can determine *a priori* what effect a given luminosity-linewidth relation would have upon incompleteness in the velocity function, but without sufficient measurements at $z \sim 1$ (which will not be possible until the DEEP2 survey is conducted), we cannot determine the resulting uncer-

tainties with precision.

Thus, rather than attempt to guess the magnitude of systematic effects that will be better understood five years from now and calculate the errors in a measurement of $\mathrm{d}N/\mathrm{d}z$ that would result, we have attempted to determine to what degree we can measure and correct for systematics using the signatures they leave on the velocity function at $z \sim 1$. In many cases, this is a pessimistic assumption; for instance, we will be able to measure our errors in determining linewidths by comparison to absorption line measurements of DEEP2 galaxies, rather than having to infer them from the velocity function alone. However, this technique has the significant advantage that we do not need to understand perfectly either the intrinsic velocity function of dark halos or any of the systematic effects to be able to assess their impact, so long as we can define "toy" models for them that replicate their major features and have the same free parameters that must be determined from the observations. For the intrinsic dark matter velocity function, we use the semi-analytic method of ND00. We have tested models of three major systematic effects expected in our measurements: the impact of baryonic infall on the circular velocities of dark halos; the effects of incompleteness at low circular velocities; and random errors in determining those circular velocities from observations. We describe our models for these in more detail below.

As a further simplification, since all physical models of either the halo velocity function or systematic effects simultaneously predict their dependence upon redshift, we determine the impact of systematics on $\mathrm{d}N/\mathrm{d}z$ measurements by treating DEEP2 as simply measuring the velocity function at $z = 1$ (the expected median redshift of the survey). This should provide the same constraints that would result from likelihood maximization over redshift and velocity simultaneously, but reduces the number of variables to be evaluated and thereby speeds computation. Thus, to determine the uncertainty resulting from one of the three systematic effects we: 1) Choose a "true" value for the free parameter α of the systematic, while using fiducial values for the other two. This defines a single probability distribution function (PDF) for galaxies (which for this purpose we define as all objects with $v_c < 300$ km s^{-1}). 2) Generate 500 Monte Carlo realizations of the velocity distribution of DEEP2 galaxies by drawing an appropriate number of objects (e.g. 10,000 for our "best bet" scenario) from this PDF. 3) For each realization, we attempt to determine the input value of the free parameter by likelihood maximization (using PDFs defined on a dense grid in α). The distribution of the best-fit values from these realizations defines the error in measuring α; this may be propagated into the uncertainty in the $\mathrm{d}N/\mathrm{d}z$ measurement. We now describe in detail the systematic effects we have investigated and the models we have used for them:

3.1. Baryonic Infall

As the baryons within a dark matter halo cool and collapse to form a galaxy, the mass distribution of the halo must respond. This changes the depth of the potential well, and thus the circular velocity in the halo on galactic scales (Blumenthal *et al.* 1986). Effectively, baryonic infall remaps a set of dark matter halos to higher circular velocity. Although the idea is not new, theoretical investigations of baryonic infall are still improving (Bullock *et al.* 2001); we expect that they will be significantly advanced by the completion of DEEP2. We thus have simply adopted a straightforward model from the literature (Gonzalez et al. 2000).

That model defines a remapping of the velocity function which combines an analytic treatment of baryonic infall with results of N-body simulations. There are three parameters in this model: λ, the galaxy spin parameter; c_{vir}, the concentration index for the Navarro, Frenk & White dark matter halos assumed by Gonzalez et al.; and m_d, the fraction of baryonic mass that forms the disk. The spin parameter λ is well-determined by N-body simulations; Gonzalez et al. assume λ=0.04, which yields results essentially identical to integrating over the GIF λ distribution (Frenk et al. 2000). The concentration index c_{vir} may also be determined from N-body simulations or semi-analytically (Bullock et al. 2000); furthermore, the effects of baryonic infall are essentially independent of c_{vir} for $c_{vir} \gtrsim 5$, a range DEEP2 galaxies at $z \sim 1$ should all fall within. Based on N-body simulations, Gonzalez et al. give a relation between c_{vir} and v_{circ} for $z = 0$, $c_{vir} \approx 13 \times \sqrt{v_{circ}/200\,\mathrm{km\ s^{-1}}}$; we take this as our guide, with prefactor taken to be 8 rather than 13 (follow-

ing the results of Bullock et al. 2000). This choice for our toy model is nearly arbitrary; appropriate simulations would be used for baryonic infall corrections to real data, but we do not require that for now.

However, the final component of the model, m_d, cannot be determined so reliably from simulations or semi-analytic models. We thus adopt it as the free parameter in our baryonic infall model, or more specifically, m_0, the prefactor in the relationship between m_d and circular velocity (taken to be 0.1 by Gonzalez et al.). This parameter has a much stronger impact on the baryonic infall remapping than λ or c_{vir}, and will be least well-known from simulations. The impact of m_0 on baryonic infall-corrected velocity functions is shown in Fig. 3.

3.2. Velocity Errors

Observations of circular velocities of DEEP2 galaxies will, of course, be subject to measurement error. Furthermore, optical spectroscopy of emmision-line objects will only determine the velocity of ionized gas at some radius within a galaxy; it is unlikely that what is measured will be identical to the dark halo circular velocity. For instance, Kobulnicky & Gebhardt (1999) found that for galaxies at $z \sim 0$, velocity measurements using O[II] and HI for the same galaxy have a $\sim$20% scatter. Because the velocity function follows a very steep power law ($n(v)dv \sim v^{-4}$) for galaxy-scale halos, such a scatter can greatly change its shape and therefore potentially affect $\mathrm{d}N/\mathrm{d}z$ measurements. For the purposes of this paper we wish to find if the amount of scatter may be determined from the observed velocity function alone.

We have adopted a simple toy model for the error in velocity measurements: $\sigma_v = \sqrt{(25\ \mathrm{kms}^{-1})^2 + (\mathrm{fv_{circ}})^2}$. The first term arises from the instrumental resolution of DEIMOS, which provides a fundamental limitation on the precision with which we can measure small velocities. The second term represents everything else that causes scatter between observed velocities and v_{circ} (after correction for baryonic infall). The results of Kobulnicky et al. suggest that the fractional error $f \sim 0.1$ locally (as the 20% scatter they found includes the effects of resolution); $f \sim 0.2$ might be reasonable for galaxies at $z \sim 1$. The effect which various values of f have upon the velocity function is shown in Fig. 4.

3.3. Incompleteness

Two types of incompleteness will affect attempts to use observable galaxies to count dark matter halos halos: incompleteness due to galaxies of a certain luminosity falling beyond the magnitude limit of the survey, and incompleteness due to dark halos which do not contain an observable galaxy. The former (which we will hereafter refer to as "luminosity incompleteness") is easy to understand: given a luminosity-linewidth relation and its scatter, one can directly calculate the fraction of galaxies for a given linewidth that will fall beyond the magnitude limit of the DEEP2 survey, and adjust the velocity function accordingly. On the other hand, knowing what fraction of dark halos with a certain circular velocity host galaxies above the surface brightness limit of a survey (or, for that matter, contain a galaxy at all) requires a full model of galaxy formation. It is not clear if this uncertainty, which we will refer to as "halo incompleteness", is an issue for the $\sim L_\star$ galaxies DEEP2 will observe or not. Unobserved low-surface brightness galaxies could also be a problem for the $z \sim 0$ comparison samples required for a $\mathrm{d}N/\mathrm{d}z$ measurement. However, the local surveys now underway will contain $5-20$ times as many galaxies as DEEP2, determining the impact of incompleteness from the observed velocity function should if anything be more effective than at $z \sim 1$.

Lacking a model for halo incompleteness, we adopt luminosity incompleteness as our toy model. Although Bullock et al. (2001) suggest that this effect will compromise measurement of $\mathrm{d}N/\mathrm{d}z$ using DEEP2 because the Tully-Fisher relation evolves with redshift, that seems highly unlikely to be a problem. With a sample of $\sim 10^4$ galaxies that have both magnitudes and linewidths, defining the slope, zero point, scatter, and evolution of a luminosity-linewidth relation should all be possible. The effect of luminosity incompleteness on the velocity function is then completely fixed, and may be corrected for directly. We demonstrate below that in fact we could accurately determine luminosity incompleteness (in the absence of halo incompleteness) using the velocity function alone. However, since we lack sufficient simulations, we presume that the impact of halo incompleteness on the velocity function would be generally simi-

lar, so that we can assess the impact of halo incompleteness by evaluating how well we can determine luminosity incompleteness from the velocity function alone. This should be generically true; it is likely that all high-circular velocity halos will contain a galaxy, and one above any surface brightness limitations of the survey at that, while smaller halos may well not. Thus, the signature of the two sorts of incompleteness is similar: full completeness for high-velocities halos, rolling over to incompleteness at lower velocities. The issues involved in halo incompleteness should be much better understood by the time the DEEP2 survey is completed, as simulations and semianalytic techniques should only improve.

For our toy model of incompleteness, we follow the results of Vogt et al. (1997) that the slope and scatter of the rest-frame B Tully-Fisher relation appear to remain unchanged to $z \sim 1$. We take as a free parameter the zero point of the relation, or equivalently v_{50}, the circular velocity (after baryonic infall) at which observations to the DEEP2 magnitude limit ($I_{AB} \sim 23.5$) will be 50% complete at $z = 1$. We thus obtain a Tully-Fisher relation:

$$M_B = -7.48 \log_{10} v_c + 40.23 - C, \qquad (3)$$

where C combines the K correction (small for conversion of B at z$\sim$0 to I at $z \sim 1$), the Hubble constant (as $-5 \log_{10} h$) and evolution of the Tully-Fisher zero point; the results of Vogt et al. suggest $C \sim 0.2 \pm 0.3$ for an $h = 0.75$ LCDM model, corresponding to $v_{50} \sim 160 \pm 15$ km s^{-1}. They found that the 0.65 mag dispersion in the Tully-Fisher relation at high redshift is consistent with being due to a 0.4 mag intrinsic scatter, a 0.2 mag scatter due to magnitude measurement errors, and a 0.47 mag scatter due to velocity errors. We apply our model incompleteness to the velocity function before adding noise, so only the first two elements of the scatter are relevant. The effect of varying v_{50} on the velocity function is shown in Fig. 5.

3.4. Resulting Errors

Given these toy models, we have generated Monte Carlo realizations of the resulting velocity functions as the parameters are varied, as described above. The net effect of these systematics in a standard scenario (m_0=0.1, $f = 0.2$, $v_{50} = 160$ km s^{-1}) is shown in Fig. 6. We expect that one-fourth to one-half of the 50,000 galaxies for which DEEP2 should obtain redshifts will provide velocity measurements. We therefore have used from 5,000 galaxies (corresponding to the total number of objects in the deeper 3HS) to 20,000 galaxies in our Monte Carlo realizations of the velocity function. Based upon the simulations, we have compiled error budgets for a determination of the volume element in three scenarios: a pessimistic one in which there are only 5,000 objects with linewidth information and the free parameters of the systematic effects take values which result in the greatest errors; a "best bet" scenario in which there are 10,000 objects and the free parameters have intermediate values; and an optimistic scenario in which there are 20,000 objects and the free parameters take favorable values. We present the resulting error budgets for a measurement of apparent density within the entire DEEP2 survey volume in Table 1.[2] In every case, the distributions of the residual errors after correction for systematics showed no major non-Gaussianities.

4. Cosmological Constraints

The DEEP2 Redshift survey will not simply measure $\mathrm{d}N/\mathrm{d}z$ at one redshift, but instead over the entire range $0.7 < z < 1.5$. To determine the resulting constraints upon cosmological parameters, we must take this into account explicitly. Because both cosmic variance and the residual errors from systematic effects after correction are essentially Gaussian, we may use a χ^2 paradigm. To simplify, we presume that DEEP2 measures $\mathrm{d}N/\mathrm{d}z$ in eight redshift bins, each covering 0.1 in z. The observed abundance in each bin will be affected by Poisson variance, by the residual errors from systematic effects after correction, and by cosmic variance.

To determine the Poisson variance in each bin, we must know the number of galaxies within it. To estimate this, we use a fit to the photometric redshift distribution of galaxies in the Hubble Deep Fields to the 1HS magnitude limit (Gwyn 1999; Lanzetta et al. 1999), which yields

[2]We have not considered the degree to which systematics may be measured or eliminated by study of the local velocity function, making our error budget a conservative one. Baryonic infall models, in particular, could be further constrained by $z \sim 0$ observations, reducing our dominant systematic uncertainty.

$\mathrm{d}N/\mathrm{d}z \propto (1+z)^{-3.25}$, and the total number of galaxies appropriate to each error scenario. To first order, residual systematic errors will affect all redshift bins in the same way. Thus, for these errors we use the same fractional error in $\mathrm{d}N/\mathrm{d}z$ for all redshift bins and presume it is completely correlated amongst them. Finally, given a cosmological model, we may calculate the cosmic variance within each redshift bin as in section 2; we treat it as completely independent between bins. In actuality, the number of objects in adjoining bins will be slightly correlated, but this is negligible compared to the uncorrelated part of the variance (or to the residual errors from systematics; the correlated part of the cosmic variance between our redshift bins is less than 10% of the total).

Given these definitions, the covariance matrix for our redshift bins is completely determined; we list the values used (for an LCDM model) in Table 2. We may then calculate χ^2 between any model and some nominal, "true" model (e.g. LCDM: $\Omega_m = 0.3$, $\Omega_Q = 0.7$, $w = -1$).[3] Observed results should be distributed as χ^2 with two degrees of freedom, so the results can be directly translated into statistical confidence contours. In Figs. 7–9 we show the results for all three error budgets. Fig. 10 shows the separate effects of cosmic variance and residual systematics. For the optimistic, best bet, and pessimistic scenarios, the error in a measurement of $w = -0.7$ will be 0.069, 0.086, or 0.11 if Ω_m is known to ± 0.025, as compared to 0.051 if Poisson errors dominated. The worse the errors on Ω_m, the less relative degradation cosmic variance and residual systematics will cause: if the error in Ω_m were 0.01, the resulting variance would be $2.2 - 6.5\times$ as large as predicted from Poisson statistics, while if it were 0.05, precision would be only $15 - 60\%$ worse than the Poisson prediction.

In Fig. 11, we present the best bet contours along with predicted or recent results for a variety of cosmological tests. Comparison to Fig. 3 of ND00 shows that even an optimistic but realistic error budget would yield poorer constraints than we previously predicted based on purely statistical errors. On the other hand, the measurement should yield much stronger limits on the dark energy than any other method available on the same timescale, at minimal marginal cost as it is a byproduct of a ground-based redshift survey that has been designed to address a number of issues in galaxy evolution and cosmology. If SNAP results are dominated by statistical uncertainties, they would yield cosmological constraints a factor of $2-3\times$ stronger than a $\mathrm{d}N/\mathrm{d}z$ measurement based on the DEEP2 galaxy velocity function alone. In the long term, the DEEP2 results would remain a valuable check on SNAP and other methods, however, as they will be subject to very different systematic errors than other cosmological tests. DEEP2 will also provide other complementary measurements of cosmological parameters through a variety of methods (e.g. by studying the abundance and velocity function of galaxy clusters within the survey volume; see Newman et al. 2001).

In summary, we have shown that the uncertainties of Newman & Davis (2000) were overly optimistic by a factor of ~ 2, as we ignored the effects of cosmic variance and had not yet tested the assumption that systematic effects could be found and corrected for based on the observed velocity function. We have demonstrated that this procedure can be implemented, though the residual errors from the correction procedure somewhat exceed the Poisson errors in a $\mathrm{d}N/\mathrm{d}z$ measurement. However, we have found no evidence that the test is compromised either by cosmic variance or any of the systematic effects considered. We must note also that our analysis has been conservative; for instance, we have not assumed that observations of the velocity function at $z \sim 0$ provides any constraints on systematic errors, nor have we considered the fact that comparison to larger-area multicolor imaging or redshift surveys could allow us to normalize out cosmic variance in the DEEP2 fields. With sufficient attention to detail, the classical $\mathrm{d}N/\mathrm{d}z$ test can provide much stronger constraints on dark energy than have ever been available before.

We wish to thank Michael Turner, whose challenge to produce a realistic error budget inspired this work, and Richard Ellis, whose inquiry about the importance of cosmic variance caused us to investigate the issue. Andrew Jaffe kindly provided

[3] We use the extension of χ^2 to a multivariate distribution with covariance: $\chi^2 = (\mathbf{n}-\mathbf{n_0})^{\mathbf{T}}\mathbf{V}^{-\mathbf{1}}(\mathbf{n}-\mathbf{n_0})$, where $\mathbf{n}$ is the vector of observations, $\mathbf{n_0}$ is the vector of true values, and $\mathbf{V}$ is the covariance matrix for $\mathbf{n_0}$. The elements of $\mathbf{V}$ are listed in Table 2.

the BOOMERANG/MAXIMA likelihood contour plotted here. We also thank Alison Coil, Christian Marinoni, and Martin White for helpful discussions. This material is based upon work supported by the National Science Foundation under Grant No. AST-0071048. This work was also made possible by equipment donated by Sun Microsystems.

REFERENCES

Bardeen, J.M, Bond, J.R., Kaiser, N., & Szalay, A. S. 1986, Ap. J., 304, 15

Benson, A.J., Pearce, F.R., Frenk, C.S., Baugh, C.M., & Jenkins, A. 1999, preprint (astro-ph/9912220)

Benson, A.J., Frenk, C.S., Baugh, C.M., Cole, S., & Lacey, C.G. 2001, preprint (astro-ph/0103092)

Blumenthal, G.R., Faber, S.M., Flores, R., & Primack, J.R. 1986, Ap. J., 301, 27

Bond, J.R. & Myers, S.T. 1996, ApJS, 103, 1

Borgani, S., Plionis, M., & Kolokotronis, V. 1999, MNRAS, 305, 866

Bryan, G.L. & Norman, M.L. 1996, Ap.J., 495, 80

Bullock, J. S. *et al.* 2000, MNRAS, 321, 559

Bullock, J. S. *et al.* 2001, Ap.J., 550, 21

Caldwell, R., Dave, R., & Steinhardt, P. 1997, Ap&SS, 261, 303

Colless, M. 1998, in *Wide Field Surveys in Cosmology*, ed. S. Colombi, Y. Mellier, & B. Raban (Paris: Editions Frontieres), 77

Cooray, A. R. & Huterer, D. 1999, Ap.J., 513, L95

Davis, M. & Faber, S. 1998, in *Wide Field Surveys in Cosmology*, ed. S. Colombi, Y. Mellier, & B. Raban (Paris: Editions Frontieres), 333

Fischer, P. *et al.* 1999, preprint (astro-ph/9912119)

Frenk, C.S. *et al.* 2000, preprint (astro-ph/0007362)

Ghigna, S., Moore, B., Governato, F., Lake, G., Quinn, T., & Stadel, J. 1999, preprint (astro-ph/991066)

Gonzalez, A.H., Williams, K.A, Bullock, J.S., Kolatt, T.S., & Primack, J.R. 2000, Ap. J., 528, 145

Gwyn, S.D.J. 1999, in ASP Conference Series 191, *Photometric Redshifts and the Detection of High Redshift Galaxies*, ed. R. Weymann, L. Storrie-Lombardi, M. Sawicki, & R. Brunner (San Francisco: ASP) 61

ogg, D.W., Cohen, J.G., & Blandford, R. 2000, Ap. J., 545, 32 ;

Hu, W., Eisenstein, D., Tegmark, M., & White, M. 1998, preprint (astro-ph/9806362)

Hubble, E. 1926, Ap.J., 64, 321

Jaffe, A. H. *et al.* 2000, PRL, 86, 3475

Jenkins, A. *et al.* 1997, in ASP Conf. Ser. 117, Dark and Visible Matter in Galaxies, ed. M. Persic & P. Salucci (San Francisco: ASP), 348

Kitayama, T. & Suto, Y. 1996a, MNRAS, 280, 638

Kitayama, T. & Suto, Y. 1996b, Ap.J., 469, 480

obulnicky, H. & Gebhardt, K. 1999, AAS, 194.0708

Kochanek, C.S., 1995, Ap.J., 453, 545

Kochanek, C.S. & White, M. 2001, preprint (astro-ph/0102334)

Lacey, C. & Cole, S. 1993, MNRAS, 262, 627

Lacey, C. & Cole, S. 1994, MNRAS, 271, 676

Lanzetta, K.M. *et al.* 1999, in ASP Conference Series 191, *Photometric Redshifts and the Detection of High Redshift Galaxies*, ed. R. Weymann, L. Storrie-Lombardi, M. Sawicki, & R. Brunner (San Francisco: ASP) 223

Loh, E.D. & Spillar, E.J. 1986, Ap.J., 307, L1

Loveday, J., *et al.* 1998, in *Wide Field Surveys in Cosmology*, ed. S. Colombi, Y. Mellier, & B. Raban (Paris: Editions Frontieres), 317

Melchiorri, A. *et al.* 1999, preprint (astro-ph/9911445)

Narayan, R. & White, S.D.M. 1988, MNRAS, 231, 97

Navarro, J. F., Frenk, C. S., & White, S. D. M. 1995, MNRAS, 275, 720

Peebles, P.J.E. 1999, *Principles of Physical Cosmology* (Princeton: Princeton University Press)

Newman, J. A. & Davis, M. 2000,Ap.J., 534 , L11

Newman, J.A., Marinoni, C., Coil, A.L., & Davis, M., PASP, accepted

Peacock, J. A., 1999, *Cosmological Physics* (Cambridge: University Press)

Perlmutter, S. *et al.* 1999, Ap.J., 517, 565

Press, W.H. & Schechter, P. 1974, Ap.J., 187, 425

Sheth, R.K., Mo, H.J., & Torment, G. 1999, preprint (astro-ph/9907024)

Steinhardt, P.J., Wang, L., & Zlatev, I. 1999, preprint (astro-ph/9812313)

Tolman, R. C. 1934, *Relativity Thermodynamics and Cosmology* (Oxford: Clarendon Press)

Turner, M. S. & White, M. 1997, Phys. Rev. D, 56, 4439

Vogt, N. P. et al. 1997, Ap. J., 479, 121

Wang, L. & Steinhardt, P.J.1998, Ap.J., 508, 483

This 2-column preprint was prepared with the AAS LaTeX macros v5.0.

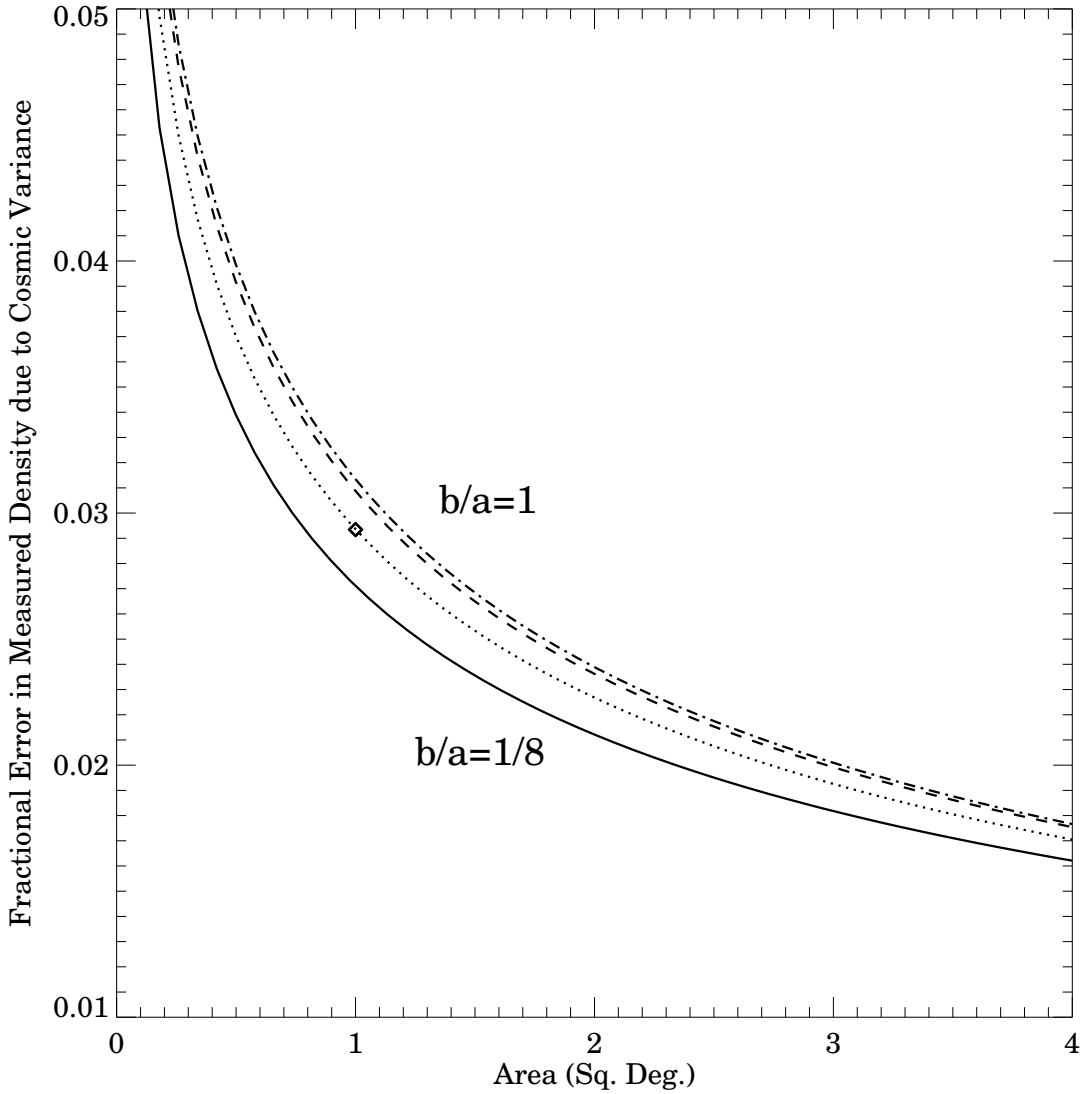

Fig. 1.— The fractional cosmic variance in a density measurement as a function of the area on the sky surveyed per field (4 fields assumed) in a volume extending from $0.7 < z < 1.5$. Curves are plotted for axis ratios $b/a = 1/8, 1/4, 1/2$ and 1. The planned geometry for the DEEP2 survey is indicated with a diamond.

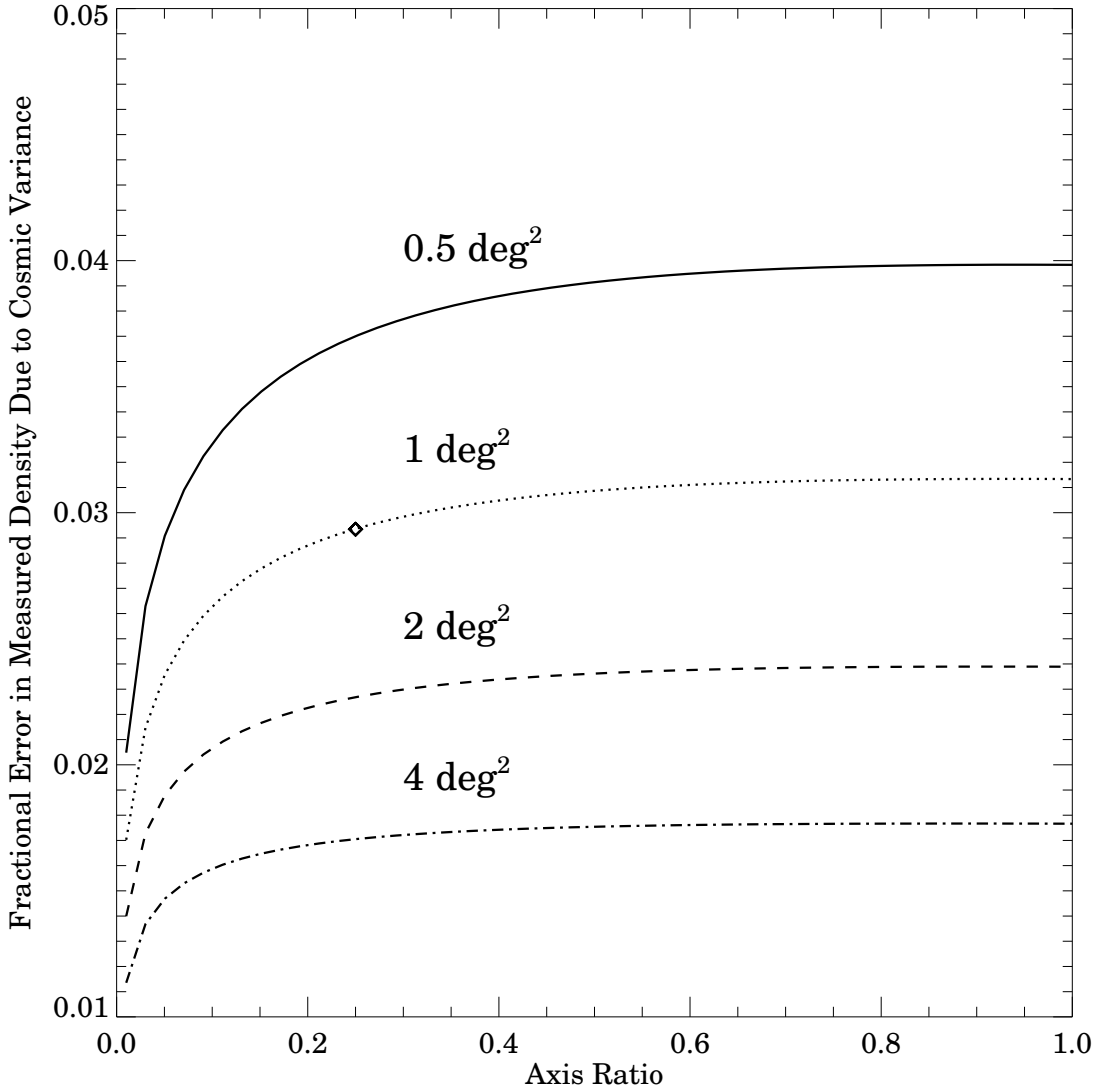

Fig. 2.— As Fig. 1, but as a function of axis ratio on the sky rather than area. Save in the most elongated cases, the amount of area surveyed per field is much more important than the axis ratio.

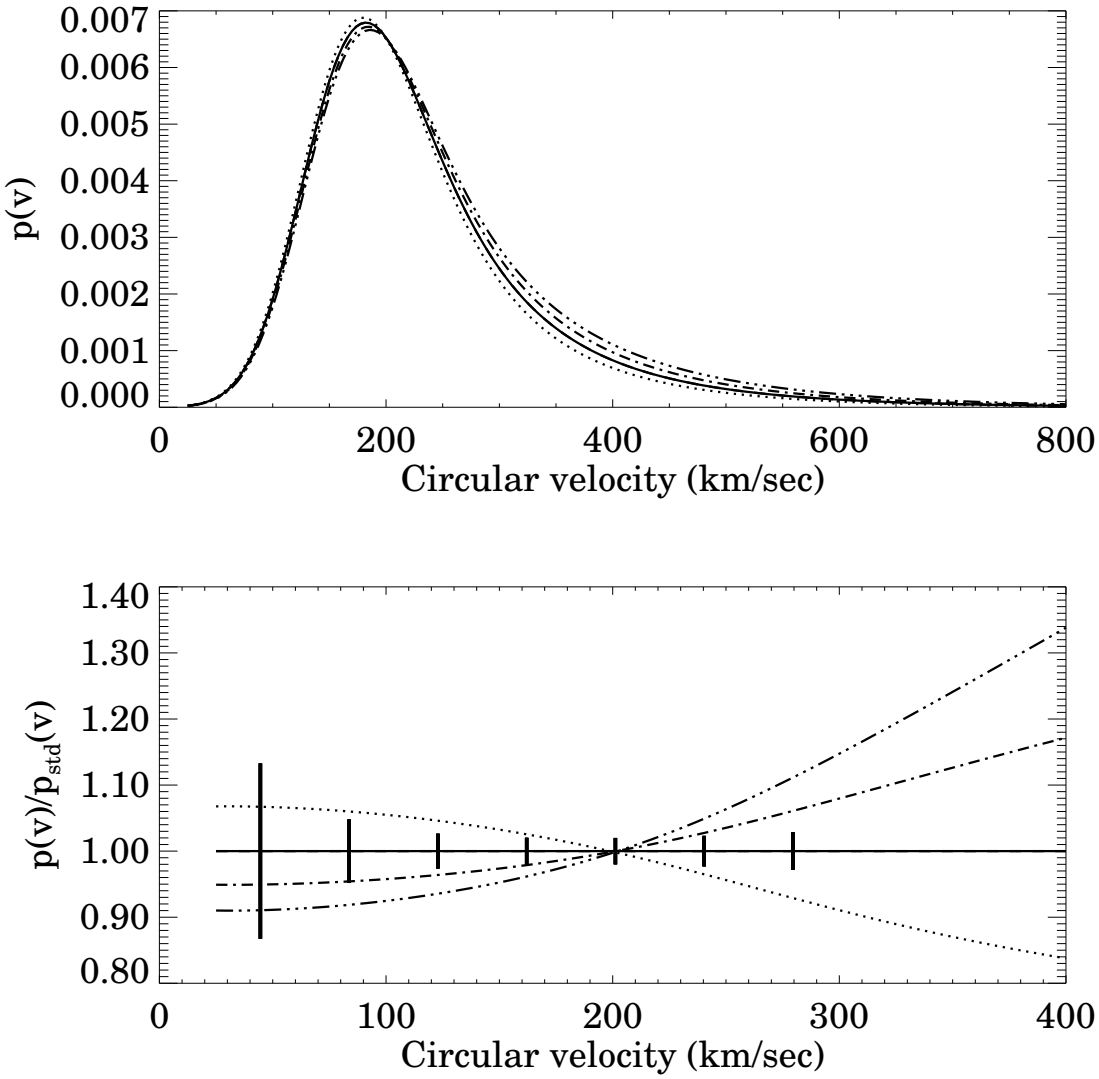

Fig. 3.— (top) The PDF for the circular velocity of dark matter halos at $z = 1$ as the disk fraction parameter m_0 is varied from 0.05 (dotted) to 0.2 (dot-dot-dot-dash). (bottom) The ratio of the PDF for varying values of m_0 to that in the fiducial model. Also plotted are expected Poisson error bars for that model if the velocity function is divided into seven bins. Compare to Figs. 4 and 5; the signatures of the three systematic effects differ strongly.

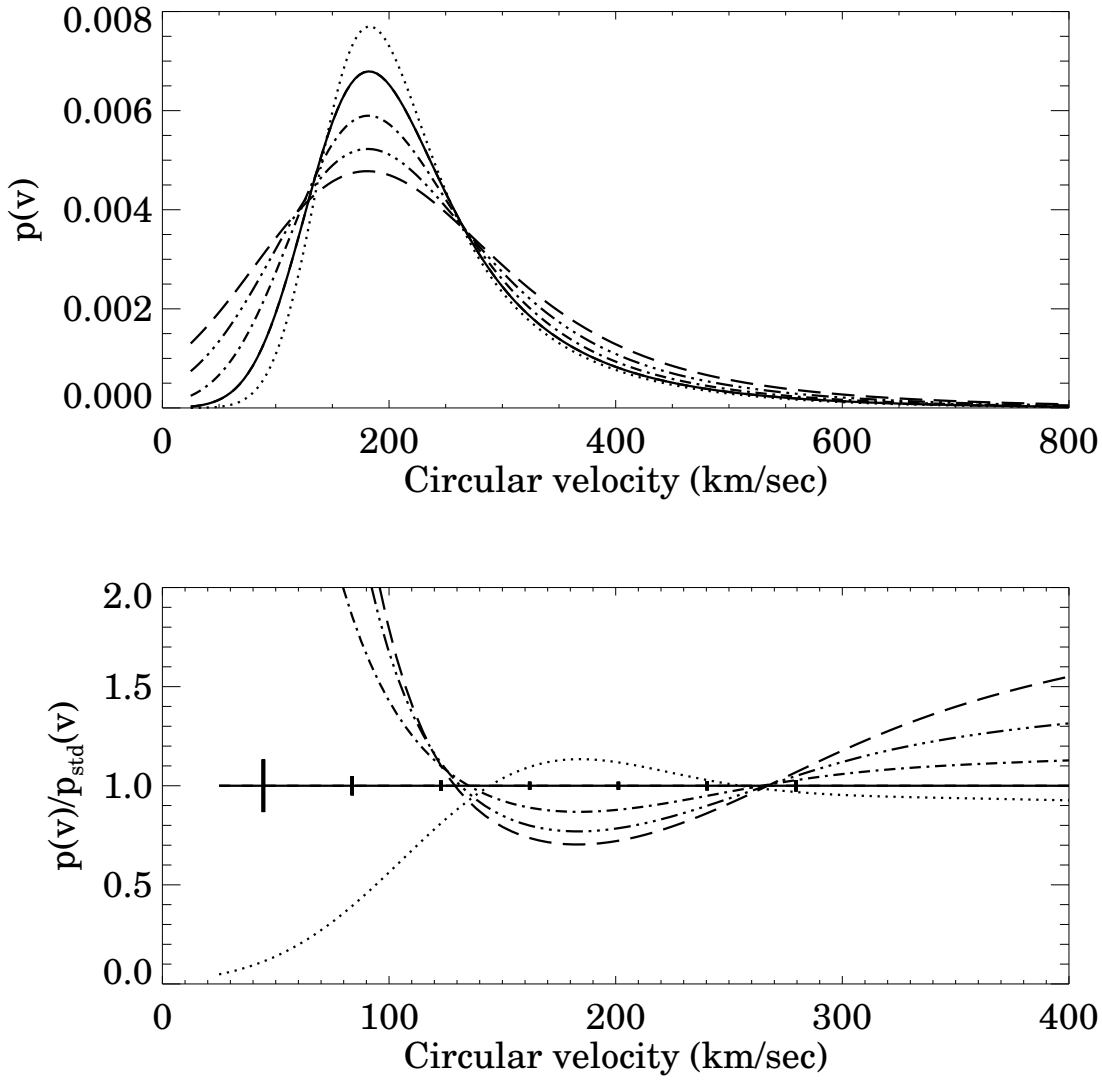

Fig. 4.— (top) As Fig. 3, but now the velocity error parameter f is varied from 0.1 (dotted) to 0.4 (dot-dot-dot-dash). (bottom) The ratio of the PDF for varying values of f to that in the fiducial model. The signature is much larger than the expected errors.

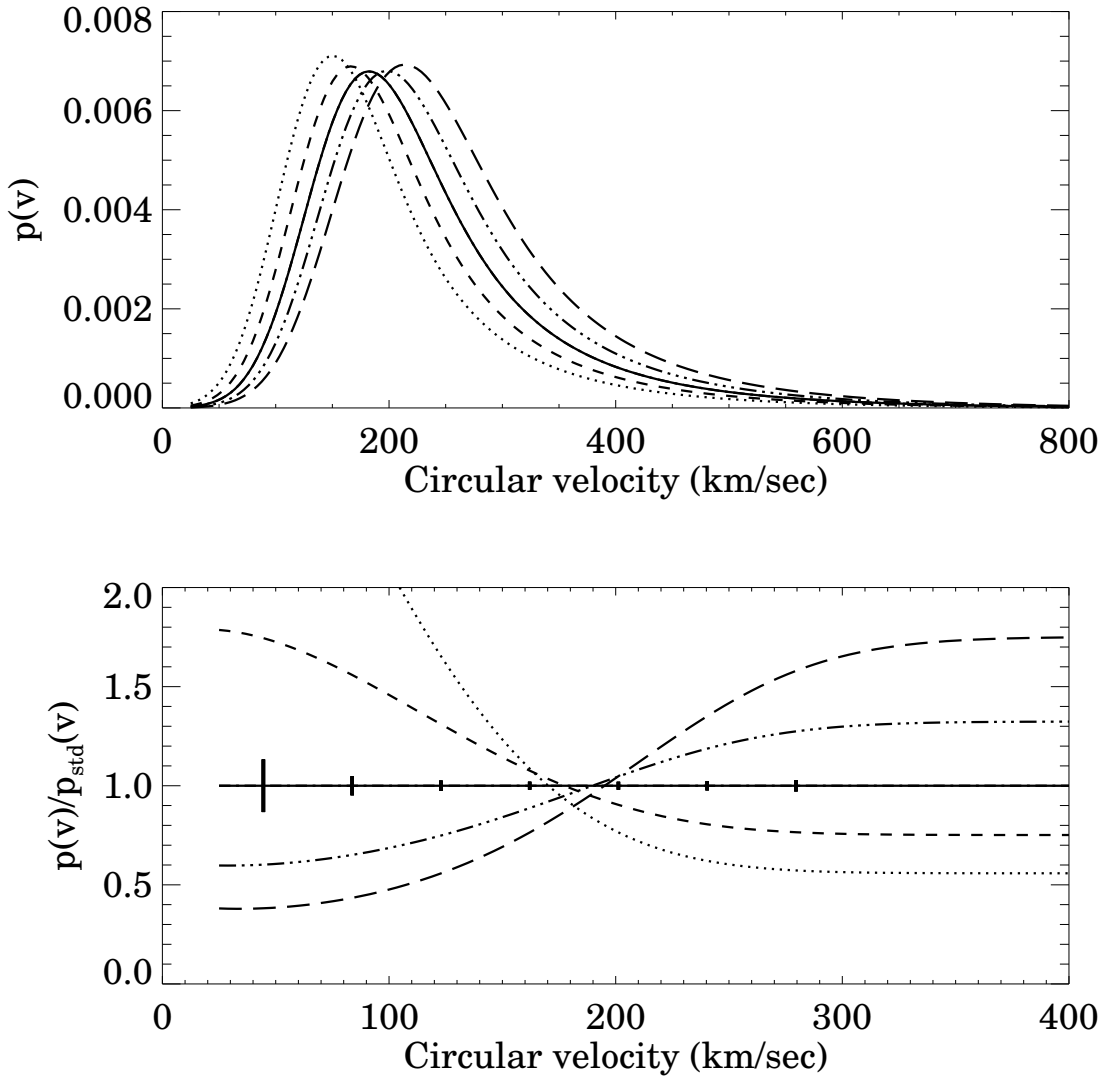

Fig. 5.— (top) As Fig. 3, but now the 50% incompleteness velocity v_{50} is varied from 130 (dotted) to 190 (dot-dot-dot-dash) km s^{-1}. (bottom) The ratio of the PDF for varying values of v_{50} to that in the standard model. Again, the signature is quite strong.

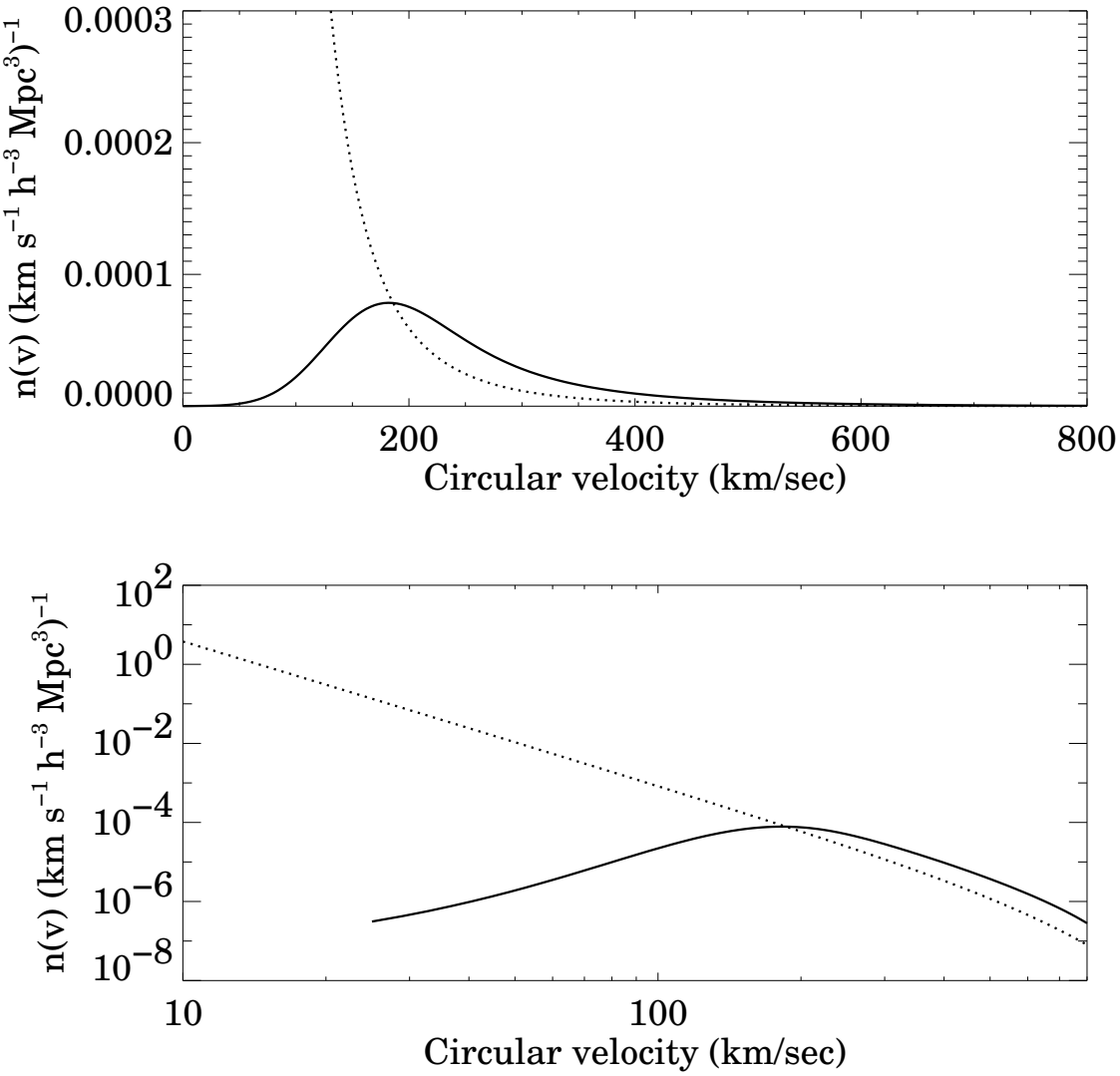

Fig. 6.— The differential circular velocity function for dark matter halos at $z = 1$, before (dotted) and after (solid) the systematic effects described in § 3 are applied. For this plot, the standard values of the free parameters ($m_0 = 0.1$, $f = 0.2$, $v_{50} = 160$ km s^{-1}) were used.

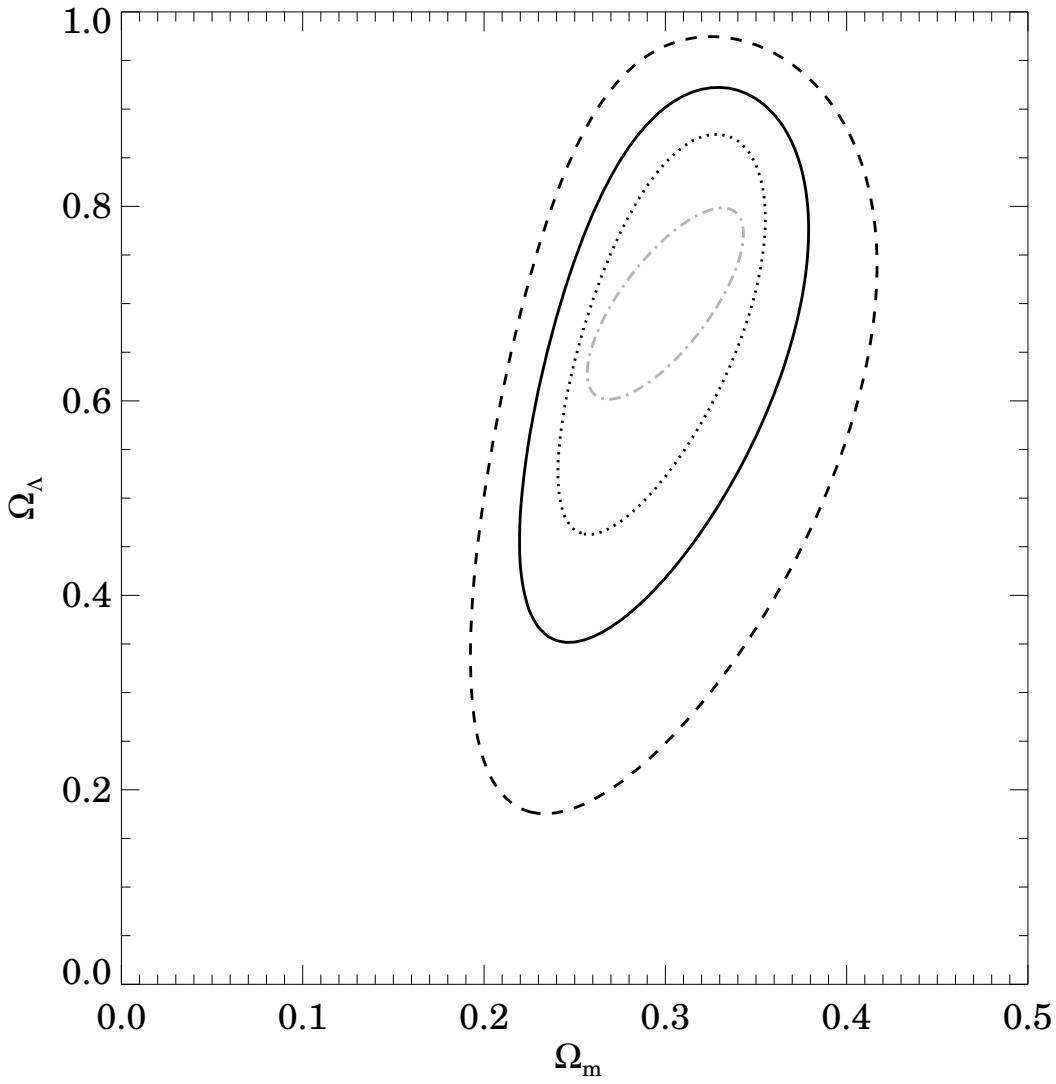

Fig. 7.— Black curves: 95% confidence constraints in the $\Omega_m - \Omega_\Lambda$ plane resulting from our three error scenarios in an $\Omega_m = 0.3$, $\Omega_\Lambda = 0.7$ model: optimistic (dotted), "best bet" (solid), and pessimistic (dashed). Also plotted for comparison is the target 95% statistical uncertainty for the SNAP project (grey, dot-dashed curve).

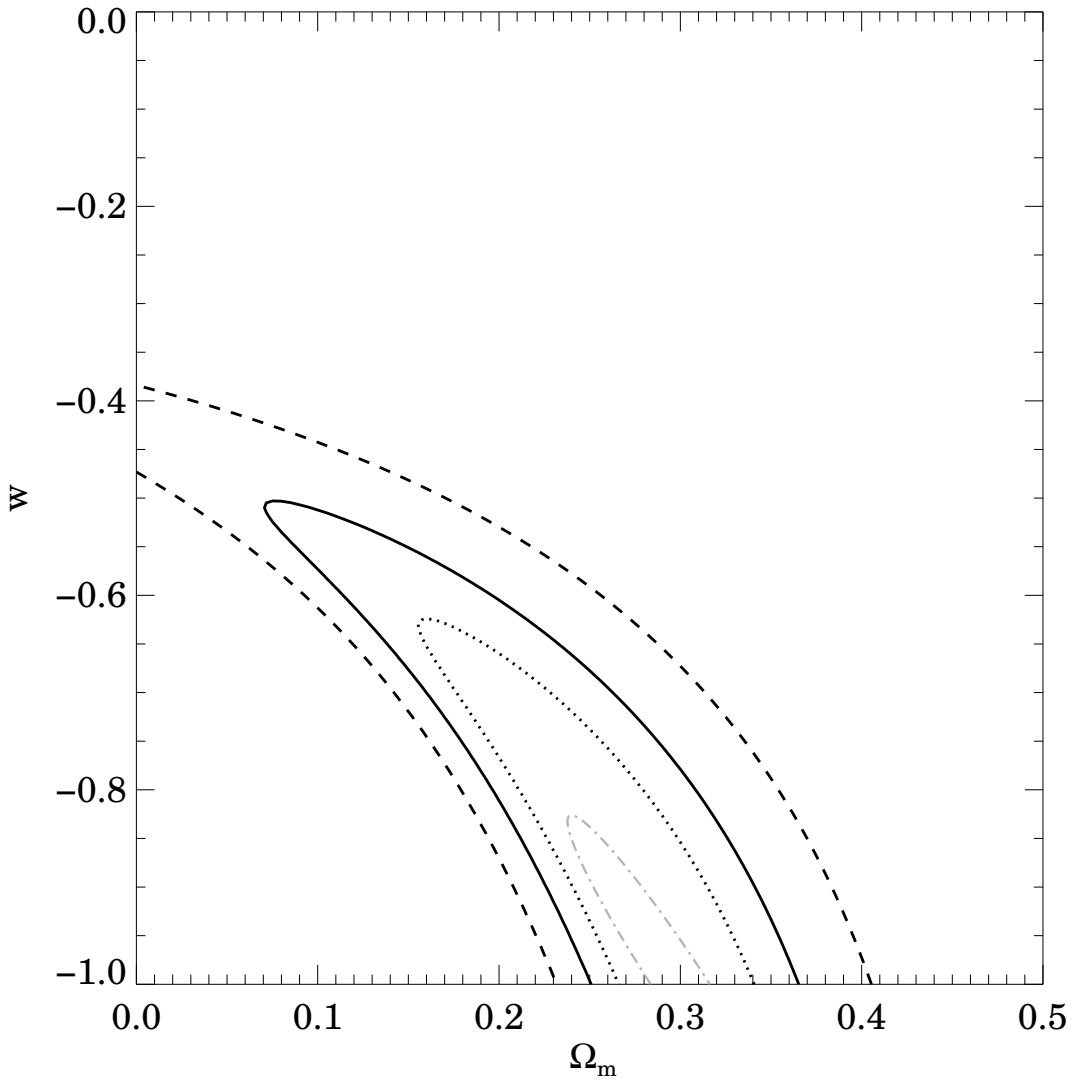

Fig. 8.— Black curves: 95% confidence constraints in the $\Omega_m - w$ plane resulting from our three error scenarios in an $\Omega_m = 0.3$, $\Omega_Q = 0.7, w = -1$ model: optimistic (dotted), "best bet" (solid), and pessimistic (dashed). Also plotted is the target 95% statistical uncertainty for the SNAP project for comparison (grey, dot-dashed curve).

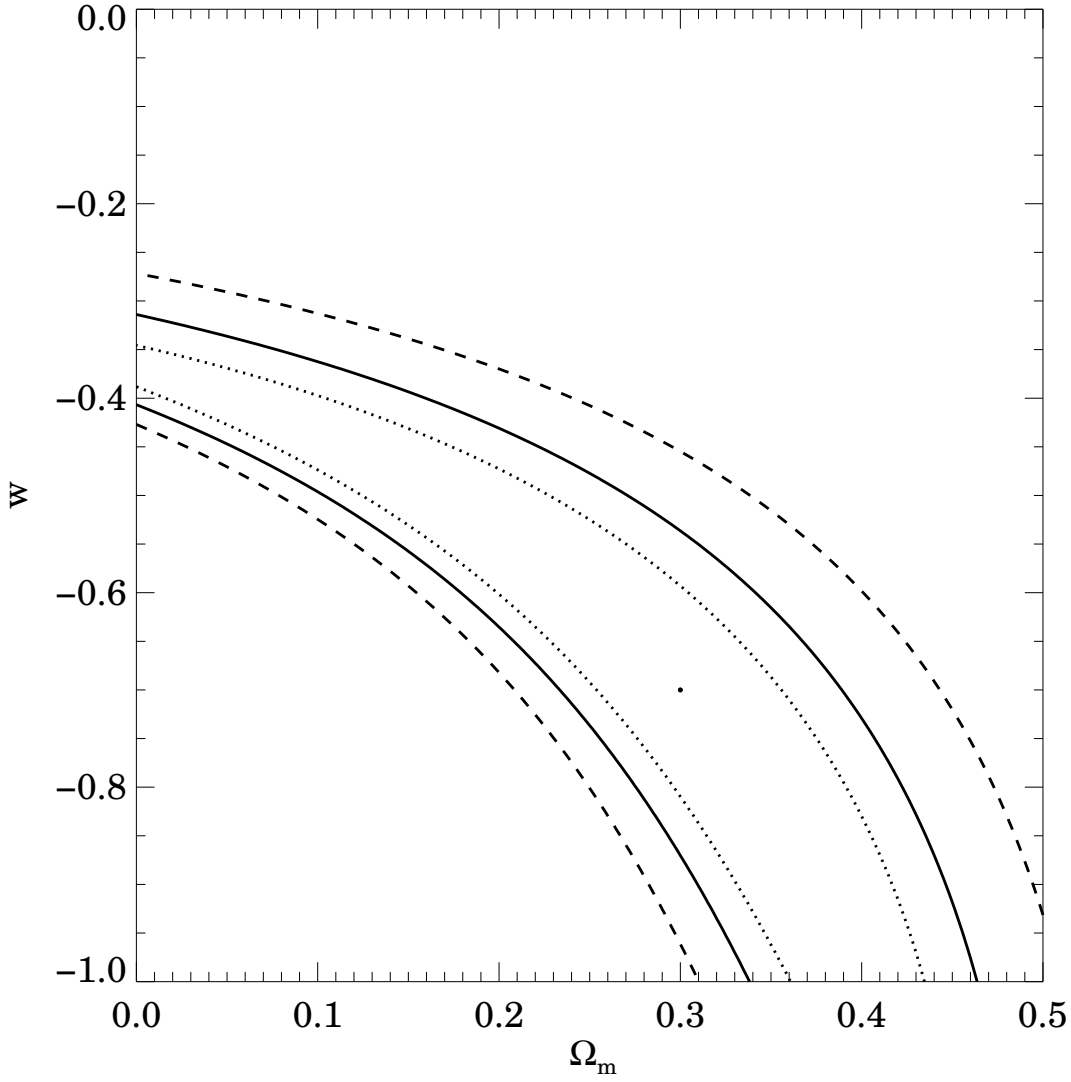

Fig. 9.— 95% confidence constraints in the $\Omega_m - w$ plane resulting from our three error scenarios n an $\Omega_m = 0.3$, $\Omega_Q = 0.7, w = -.7$ model: optimistic (dotted), "best bet" (solid), and pessimistic (dashed).

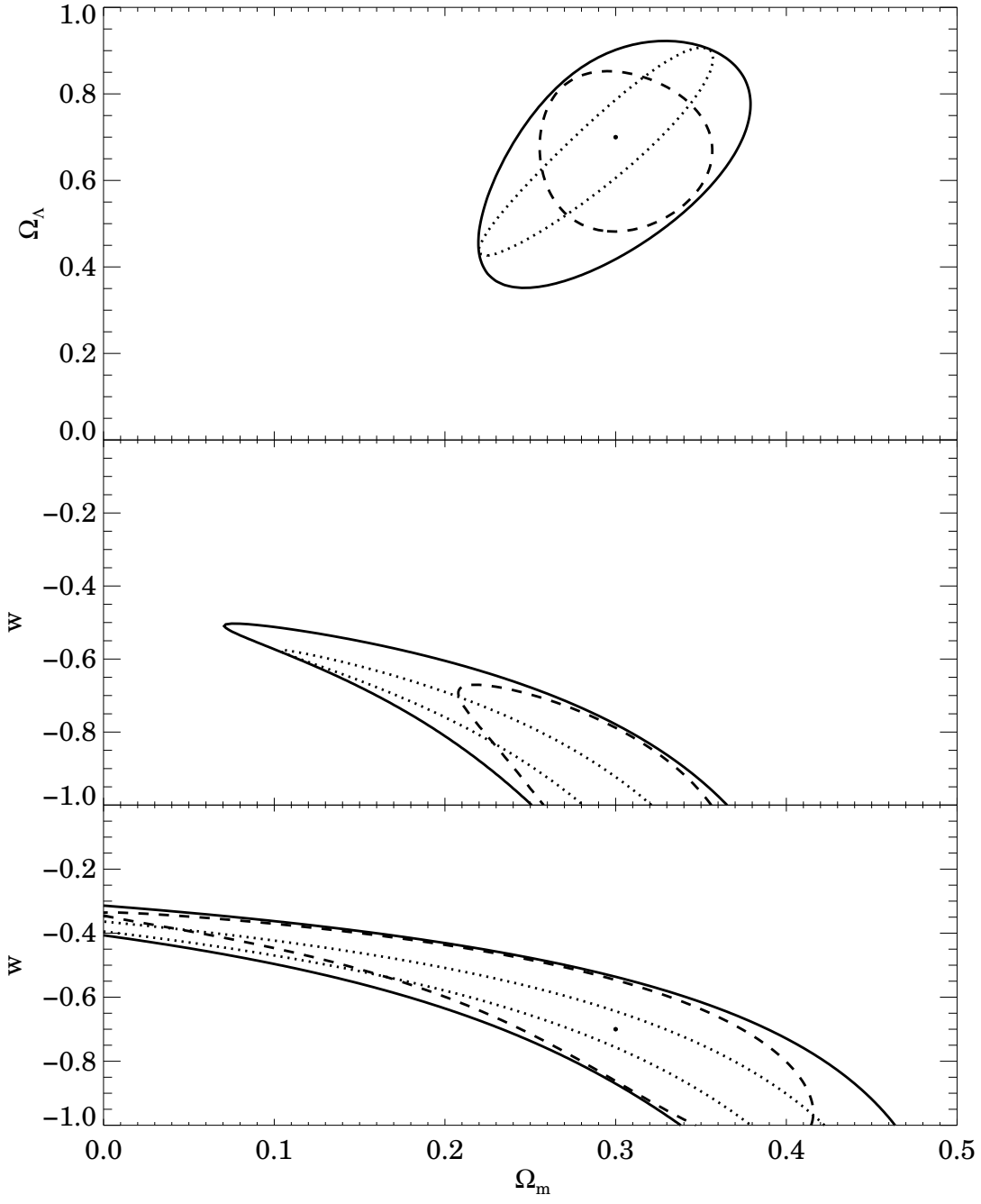

Fig. 10.— The best bet contours from the previous three figures (solid black curves), along with curves indicating what the constraints with zero systematic errors (dotted curves) or zero cosmic variance (dashed curves). (Top) Constraints in the $\Omega_m - \Omega_\Lambda$ plane for an $\Omega_m = 0.3$, $\Omega_\Lambda = 0.7$ model. (Middle) Constraints in the $\Omega_m - w$ plane for a model with $\Omega_m = 0.3$, $w = -1$. (Bottom) As the middle panel, but for a model with $w = -0.7$. In most cases, the effects of both cosmic variance and systematic effects are of comparable importance.

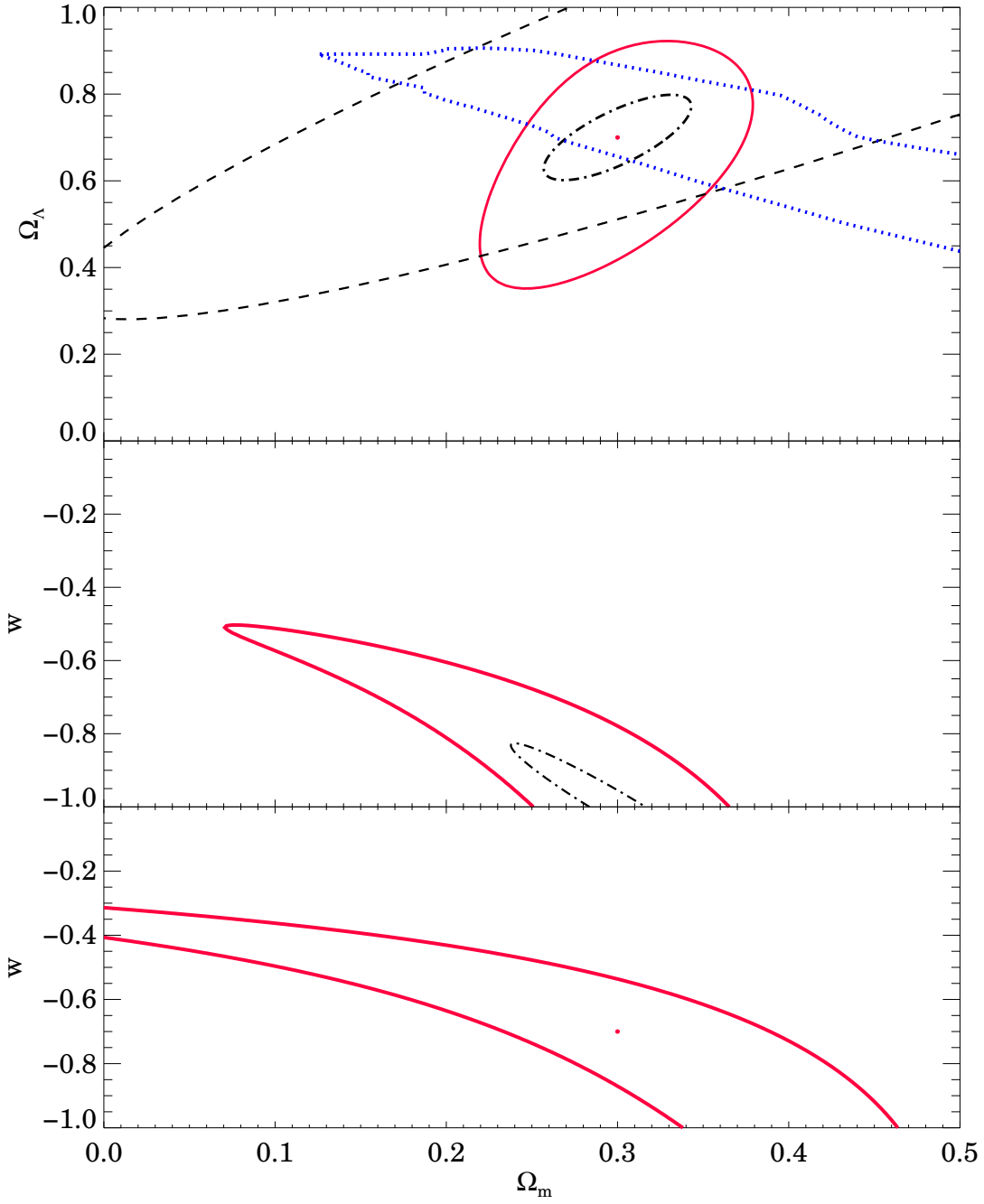

Fig. 11.— The best bet contours from the previous three figures (solid red curves), along with other current or near-future measurements. (Top) Plotted constraints in the $\Omega_m - \Omega_\Lambda$ plane include the current 68% SNe Ia results (Perlmutter et al. 1999; large black dashed curve) and BOOMERANG/MAP measurements (Jaffe et al. 2000; blue dotted curve), along with (for an $\Omega_m = 0.3$, $\Omega_\Lambda = 0.7$ model) the 95% SNAP target statistical uncertainty (black dot-dash curve). (Middle) Potential measurements in the $\Omega_m - w$ plane for a model with $\Omega_m = 0.3$, $w = -1$. In addition to our "best bet" scenario, the SNAP target statistical uncertainty is shown (black dot-dashed curve). (Bottom) As the middle panel, but for a model with $w = -0.7$.

TABLE 1
ERROR BUDGETS FOR DENSITY MEASUREMENTS FROM DEEP2

	Error Scenario:					
	Pessimistic		Best Bet		Optimistic	
Error Source	Fractional Error (Parameter Value)					
Counting Statistics	0.014	(N=5000)	0.010	(N=10000)	0.007	(N=20000)
Cosmic Variance	0.022	($\sigma_8 = 0.723$)	0.018	($\sigma_8 = 0.600$)	0.014	($\sigma_8 = 0.474$)
Baryonic Infall[1]	0.080	($m_0 = 0.05$)	0.050	($m_0 = 0.1$)	0.033	($m_0 = 0.2$)
Velocity Errors[1]	0.012	($f = 0.4$)	0.002	($f = 0.2$)	0.001	($f = 0.2$)
Incompleteness[1]	0.021	($v_{50} = 175$)	0.014	($v_{50} = 160$)	0.009	($v_{50} = 145$)

[1]Residual error when the observed velocity function is used to measure and remove the effect

TABLE 2
COVARIANCE MATRIX ELEMENTS

Element[1]	Pessimistic	Best Bet	Optimistic
1,1	0.00313 n_1^2	0.00620 n_1^2	0.01203 n_1^2
2,2	0.00307 n_2^2	0.00611 n_2^2	0.01196 n_2^2
3,3	0.00303 n_3^2	0.00608 n_3^2	0.01197 n_3^2
4,4	0.00303 n_4^2	0.00609 n_4^2	0.01205 n_4^2
5,5	0.00304 n_5^2	0.00614 n_5^2	0.01220 n_5^2
6,6	0.00308 n_6^2	0.00623 n_6^2	0.01241 n_6^2
7,7	0.00313 n_7^2	0.00635 n_7^2	0.01267 n_7^2
8,8	0.00320 n_8^2	0.00649 n_8^2	0.01298 n_8^2
$i, j, i \neq j$	0.00123 $n_i n_j$	0.00305 $n_i n_j$	0.00719 $n_i n_j$

[1]These are elements of the covariance matrix for n_i, where n_i is the number of objects in the ith redshift bin. An LCDM model with $\Omega_m = 0.3, \Omega_\Lambda = 0.7, w = -1$ has been used. The first bin extends from $z = 0.7$ to 0.8, the second from 0.8 to 0.9, etc. If f_{CV} is the fractional error from cosmic variance in a bin, f_{count} that from counting statistics, and f_{sys} that from residual systematics (combined in quadrature), the diagonal elements of the covariance matrix will be $(f_{CV}^2 + f_{count}^2 + f_{sys}^2)n_i^2$, while the off-diagonal elements will be $f_{sys}^2 n_i n_j$.